

Stereochemistry of Molecular Figures-of-Eight

Megan M. Boyle,^[b] Jeremiah J. Gassensmith,^[b] Adam C. Whalley,^[b] Ross S. Forgan,^[b]
Ronald A. Smaldone,^[b] Karel J. Hartlieb,^[b] Anthea K. Blackburn,^[b]
Jean-Pierre Sauvage,^{*,[a, b]} and J. Fraser Stoddart^{*,[b, c]}

Abstract: A *trans* isomer of a figure-of-eight (Fo8) compound was prepared from an electron-withdrawing cyclobis(paraquat-*p*-phenylene) derivative carrying *trans*-disposed azide functions between its two phenylene rings. Copper(I)-catalyzed azide-alkyne cycloadditions with a bispropargyl derivative of a polyether chain, interrupted in its midriff by an electron-donating 1,5-dioxynaphthalene unit acting as the template to organize the reactants prior to the onset of two click reactions, afforded the Fo8 compound with C_i symme-

try. Exactly the same chemistry is performed on the *cis*-bisazide of the tetracationic cyclophane to give a Fo8 compound with C_2 symmetry. Both of these Fo8 compounds exist as major and very minor conformational isomers in solution. The major conformation in the *trans* series, which has been characterized by X-ray crystallography, adopts

Keywords: click chemistry • donor-acceptor systems • rotaxane • topology • X-ray diffraction

a geometry which maximizes its C–H...O interactions, while maintaining its π ... π stacking and C–H... π interactions. Ab initio calculations at the M06L level support the conformational assignments to the major and minor isomers in the *trans* series. Dynamic ¹H NMR spectroscopy, supported by 2D ¹H NMR experiments, indicates that the major and minor isomers in both the *cis* and *trans* series equilibrate in solution on the ¹H NMR timescale rapidly above and slowly below room temperature.

Introduction

The field of chemical topology^[1] has enabled the design of molecular representations of mathematical topologies and aided in the syntheses and analyses of both topologically trivial and non-trivial chemical motifs. Often, molecular recognition and self-assembly are used to template^[2] the formation of higher-order architectures by stabilizing inclusion complexes through interactions such as hydrogen bonding and π - π stacking. Importantly, this use of templates can be employed to direct the location and geometry of covalent

bond formation in order to tailor the way portions of a molecule orient themselves with respect to each other, allowing chemists to create both single-station and switchable mechanically interlocked molecules (MIMs).^[3] These methods result in single molecules composed of several components held together through mechanical bonds, for example, catenanes,^[4] rotaxanes,^[5] and Borromean rings.^[6] Self-complexing compounds^[7] and pretzelanes^[8] are synthesized by means of *intramolecularly* template-directed protocols. Here, we describe the synthesis of isomers of a molecular figure-of-eight^[9] (Fo8) using an *intermolecularly* templated protocol.

The electron-deficient cyclophane,^[10] cyclobis(paraquat-*p*-phenylene) (CBPQT⁴⁺), has been employed as the molecular host to encircle an electron-rich guest en route to obtaining^[4a, 11] many different architectures. Traditionally, this family of cyclophanes is synthesized through a template-directed approach.^[12] Introducing various functionalities onto the xylylene units of the cyclophane precursors can potentially hinder cyclophane formation, depending on the electronic and steric nature of the functional group. Modification of CBPQT⁴⁺ with a *single* functional handle on one of the phenylene rings is possible and does not alter significantly the binding capabilities of the cyclophane. Although this approach has been used to synthesize complex molecules, such as pretzelanes,^[8, 13] polymers,^[14] and linked nanoparticles,^[15] further modification of CBPQT⁴⁺ with *multiple* functional handles has remained an elusive target until recently, though it does provide access to new topologies that have been unattainable thus far. Although a two-armed self-

[a] Prof. J.-P. Sauvage
Institut de Science et d'Ingénierie Supramoléculaires
Université de Strasbourg
8 allée Gaspard Monge, F-67000 Strasbourg (France)
E-mail: jpsauvage@unistra.fr

[b] Dr. M. M. Boyle, Dr. J. J. Gassensmith, Dr. A. C. Whalley,
Dr. R. S. Forgan, Dr. R. A. Smaldone, Dr. K. J. Hartlieb,
A. K. Blackburn, Prof. J.-P. Sauvage, Prof. J. F. Stoddart
Center for the Chemistry of Integrated Systems
and Department of Chemistry, Northwestern University
2145 Sheridan Road, Evanston, IL 60208-3133 (USA)
Fax: (+1) 847-491-1009
E-mail: stoddart@northwestern.edu

[c] Prof. J. F. Stoddart
NanoCentury KAIST Institute and Graduate School of EEWS
(WCU)
Korea Advanced Institute of Science and Technology (KAIST)
373-1, Guseong Dong, Yuseong Gu, Daejeon 305-701 (Republic of Korea)

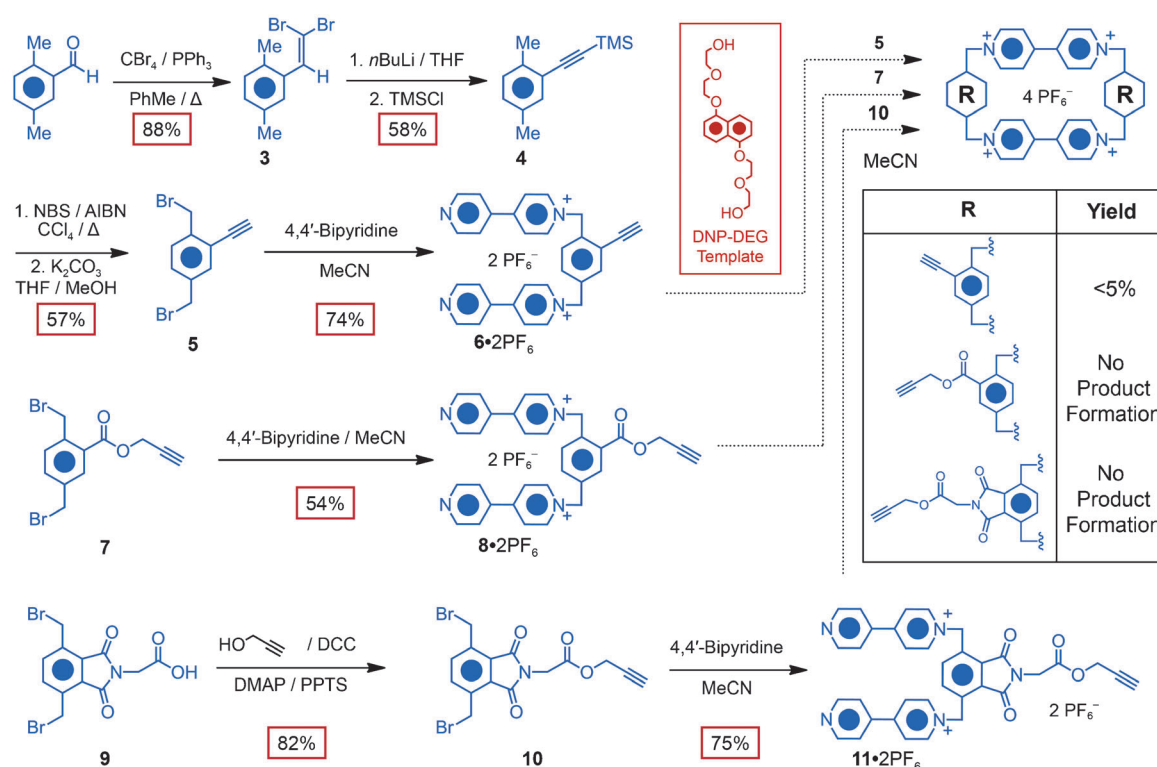
Supporting information for this article is available on the WWW under <http://dx.doi.org/10.1002/chem.201202070>.

complexing rotaxane^[7b] has been synthesized containing a bisfunctionalized cyclophane formed through an intramolecular template approach, an uncomplexed bisfunctional cyclophane has not been isolated and characterized until very recently. A straightforward example of a topology obtainable by incorporating bisfunctionality onto the CBPQT⁴⁺ ring is called a self-complexing [1]rotaxane, or the molecular figure-of-eight^[9,16] (Fo8), in which a guest is threaded through the cavity and linked covalently to the host twice. Herein, we report the 1) design, 2) synthesis, and 3) characterization of the molecular Fo8, **1**·4PF₆ via the cyclophane intermediate **2**·4PF₆, and discuss 4) the resulting stereochemical implications and consequences. Although this research has been the subject of a preliminary communication,^[9] the recent advent of a crystal structure of one of the Fo8 compounds has encouraged us to revise our opinion on the geometry of the major conformation of the compound present in solution.

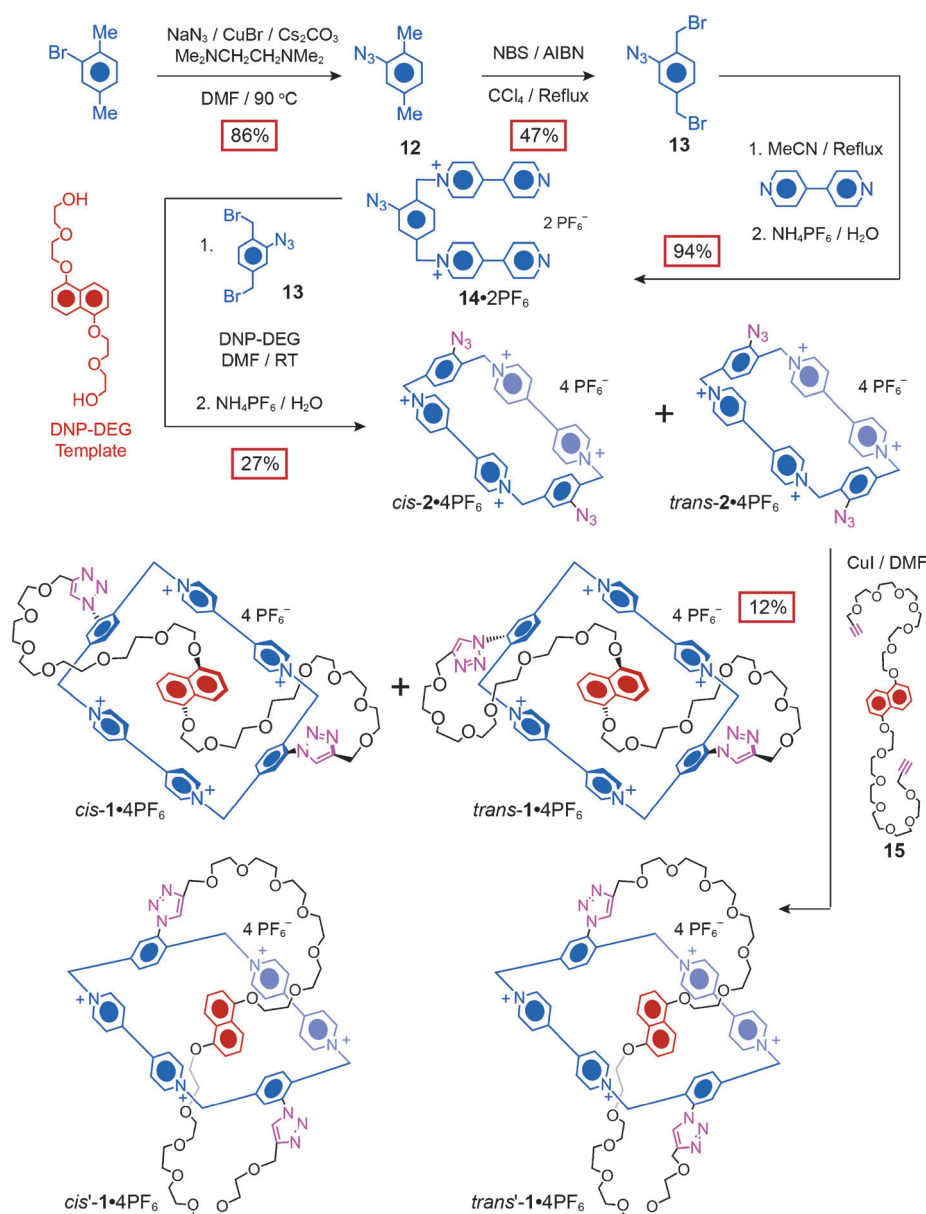
Results and Discussion

In an effort to assemble a self-complexing [1]rotaxane, several bisfunctional CBPQT⁴⁺ derivatives (Scheme 1) were considered as lead compounds based on functional groups that had previously been incorporated^[7b,17] into monofunctionalized derivatives of CBPQT⁴⁺. While in all the exam-

ples we considered, a dicationic precursor could be synthesized and characterized, the final ring-closing step could not be performed in all but one case. The synthetic steps necessary to reach the desired cyclophanes, and the yields (if any) of the final ring-closing steps in the template-directed formation of the tetracationic cyclophane are shown in Scheme 1. Initial attempts were based on appending alkynes to the cyclophane to prepare CBPQT⁴⁺ for copper(I)-catalyzed azide-alkyne cycloaddition^[18] (CuAAC). In the context of CuAAC, attachment of azides, rather than alkynes, to the cyclophane was pursued subsequently. It was found that the azide-modified aryl dibromide **13** was the only suitable substrate and fortunately it afforded (Scheme 2) the highest yield of cyclophane in a minimum number of synthetic steps. All of the alkyne-based modifications disrupted the mechanism of cyclophane formation so significantly that negligible quantities of product were formed, even when the final template-driven ring-closing step was performed under ultra-high pressure (15 kbar). Because the azide group is, comparatively speaking, sterically small and electronically benign,^[19] it allows retention of the binding affinity of the tetracationic cyclophane for electron-rich guests, such that good yields of the cyclophane can still be obtained. Beginning with the commercially available 2-bromo-1,4-dimethylbenzene, an Ullman-type coupling was performed in order to afford compound **12**, which was brominated to give **13**. Reaction of **13** with an excess of 4,4'-bipyridine afforded the



Scheme 1. A description of the synthetic attempts to form a bisfunctional cyclophane based on the CBPQT⁴⁺ ring. Three targets were initially designed incorporating alkynes for further functionalization. Precursors **6**·2PF₆, **8**·2PF₆, and **11**·2PF₆ were synthesized successfully, but the final ring-closing step in each case yielded little or no product. This result is most likely because functionalization of the aryl group weakened significantly the ability of a transition state to recognize a guest and thus a template approach could not be utilized to form the final cyclophanes.



dicationic precursor $14\cdot 2\text{PF}_6$, which could be reacted with another equivalent of **13** in the presence of an electron-rich template to afford^[20] two inseparable isomers of $2\cdot 4\text{PF}_6$ —*cis*- $2\cdot 4\text{PF}_6$, in which both azides are pointing toward the same bipyridinium unit, and *trans*- $2\cdot 4\text{PF}_6$, in which the azides are pointing toward opposite bipyridinium units.

The synthesis of the molecular Fo8 is templated by the strong host-guest complex that is formed between the π -electron-deficient cyclophane $2\cdot 4\text{PF}_6$ and the π -electron-rich guest **15**. Functionalization of CBPQT^{4+} at both xylylene linkers is expected to alter the binding properties of the host towards guests. In order to probe the ability of $2\cdot 4\text{PF}_6$ to bind with electron-rich substrates, the association constants (K_a values) and other thermodynamic data for the complexation of the bisfunctionalized host with electron-rich guests have been obtained experimentally using isothermal titration calorimetry (ITC) and compared (Table 1) to a similar monofunctionalized cyclophane (in which only one xylylene linker contains the azide function— $\text{CBPQT}^{4+}\text{-N}_3$) and the free unsubstituted CBPQT^{4+} . For ITC isotherms, see the Supporting Information. In the case of a 1,5-dioxynaphthalene (DNP) unit functionalized with hexaethylene glycol (HEG) chains at each phenolic hydrox-

Table 1. Thermodynamic binding data corresponding to the complexation between various CBPQT^{4+} -based hosts and both 1) DNP-HEG-dA guest and 2) TTF-HEG-dA guest in MeCN as determined by isothermal titration microcalorimetry at 298 K.^[a]

	DNP-HEG-dA Guest				TTF-HEG-dA Guest			
	$\Delta H^{[b]}$	$\Delta S^{[c]}$	$\Delta G^{[d]}$	$K_a^{[e]}$	$\Delta H^{[b]}$	$\Delta S^{[c]}$	$\Delta G^{[d]}$	$K_a^{[e]}$
CBPQT^{4+}	-15.34 ± 0.03	-29.3 ± 0.1	-6.61 ± 0.04	67.5 ± 1.1	-12.50 ± 0.06	-16.7 ± 0.5	-7.52 ± 0.16	333 ± 26
$\text{CBPQT}^{4+}\text{-N}_3$	-14.38 ± 0.04	-28.6 ± 0.9	-5.86 ± 0.29	19.3 ± 0.3	-12.20 ± 0.07	-16.7 ± 0.2	-7.22 ± 0.09	195 ± 14
$\text{CBPQT}^{4+}\text{-(N}_3)_2$	-12.65 ± 0.01	-25.2 ± 0.2	-5.14 ± 0.13	5.71 ± 0.1	-11.94 ± 0.05	-16.5 ± 0.2	-6.98 ± 0.08	141 ± 7

[a] All ITC measurements were performed in dry, degassed MeCN at 298 K. A solution of CBPQT^{4+} , $\text{CBPQT}^{4+}\text{-N}_3$, or $\text{CBPQT}^{4+}\text{-(N}_3)_2$ (0.5 mM) was used as the host solution. Solutions of DNP-HEG-dA or TTF-HEG-dA (5 mM unless otherwise stated) were added by successively injecting 10 μL of a titrant solution over 20 s (23 times) with a 300 s interval between each injection. Experiments for each host and guest were repeated three times. [b] [kcal mol⁻¹]. [c] [cal mol⁻¹ K⁻¹]. [d] [kcal mol⁻¹]. [e] $\times 10^3$ [M⁻¹].

yl group, and terminated with alkynes (DNP-HEG-dA), going from the unfunctionalized cyclophane to a monosubstituted one and subsequently to a difunctionalized one results in a decrease of the K_a value between the host and guest by no more than an order of magnitude. Furthermore, in the case of another electron-rich guest, a bis(methylene)-substituted tetrathiafulvalene (TTF) similarly extended at both functional groups with hexaethylene glycol chains and terminated with alkynes (TTF-HEG-dA), the binding affinity is only decreased ever so slightly. Hence, the binding capabilities of the host $2\cdot4\text{PF}_6$ remain sufficiently strong, encouraging us to proceed with further experiments.

The DNP-based derivatives, possessing a sufficiently high K_a value when complexed with cyclophane $2\cdot4\text{PF}_6$, yet lacking the isomer complications common to TTF derivatives,^[21] make them ideal guests for the synthesis of a molecular Fo8. Using a mixture of the CBPQT⁴⁺ bisazides and DNP-HEG-dialkyne derivative **15**, CuAAC was employed to link the complex covalently to produce (Scheme 2) the Fo8 ($1\cdot4\text{PF}_6$). As a result of using a mixture of the two isomers of $2\cdot4\text{PF}_6$, the product was a mixture of two isomers. Recycling reverse-phase high-performance liquid chromatography (RP-HPLC) was used in order to separate and characterize fully^[9] two very similar compounds—*cis*- 1^{4+} , in which both triazoles are pointing toward the same bipyridinium unit, and *trans*- 1^{4+} , in which the triazoles are pointing toward opposite bipyridinium units.

Crystals of *trans*- $1\cdot4\text{TFA}$ (Figure 1 a), grown from Me_2CO using slow vapor diffusion of Et_2O , possess a solid-state structure (Figure 1 b) which aids the identification of the geometry of the Fo8—the solid-state structure is found to be in contrast to *trans*'- 1^{4+} , the structure (Scheme 2) previously proposed,^[9] in terms of its constitution and conformation. The compound crystallizes in the triclinic space group $P\bar{1}$ with one half of a molecule, two CF_3COO^- counterions, and two MeCN solvent molecules in the asymmetric unit. The complete molecule was generated by an inversion operation through the center of the molecule at the origin, in concert with its proposed C_i point group. The CBPQT⁴⁺ portion of the molecule sits flat along a plane through the corner methylenes and, as with the majority of solid-state structures^[4q,22] containing CBPQT⁴⁺, the pyridinium rings are twisted slightly from planarity, with an angle of 16° present between neighboring heterocycles. The 1,2,3-triazole rings bound to each xylyl moiety are twisted from the plane of the xylene rings by 47° , while the nitrogen atoms of the triazole functionality are directed towards the center of the molecule. The hexaethylene glycol chains are then directed around the outside of the CBPQT⁴⁺ moiety and connected to the DNP unit, which sits inside the CBPQT⁴⁺ ring. As a result of the generation of the full structure from the inversion operation, the glycol chains are located on opposite sides of the molecule. Multiple C–H...O interactions (Figure 1 c) are present between CBPQT⁴⁺ and the oxygen atoms of the glycol chains, which act to hold the polyether loops in close proximity around the macrocycle. These interactions range in distance from 3.40 \AA in the case of C–H...O (pyridyl H to

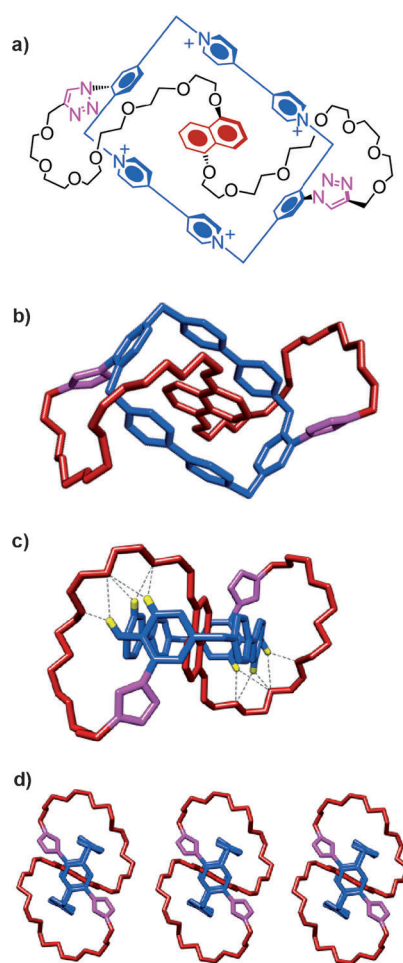


Figure 1. The structural formula a) of *trans*- 1^{4+} and a tubular representation of its b) X-ray crystal structure (non-interacting H atoms and anions have been omitted for clarity). Note that in the solid-state structure, the calculated energetically favorable orientation of the dioxynaphthalene core is, in fact, observed. The C–H...O interactions which hold the Fo8 in this orientation are denoted in c). The X-ray crystal packing d) shows that parallel sheets of *trans*- 1^{4+} are found in the crystal structure.

glycol O closest to the triazole ring), to 2.98 \AA in the case of C–H...O (methylene H to glycol O in the middle of the chain). Bifurcated interactions between pyridyl H and the glycol chain closest to the DNP unit are also present. These noncovalent bonding interactions are known^[23] to impart significant stability to MIMs, such as $1\cdot4\text{PF}_6$, and are the most likely driving force behind the arrangement of the polyether loops such that they connect DNP and triazole units located on *opposite* faces of the Fo8 rather than on the *same* face. The DNP unit sits inside the CBPQT⁴⁺ ring so that C–H... π interactions (3.46 \AA) are present between the *peri*-hydrogen atoms on the DNP unit with both the aromatic xylylene components of CBPQT⁴⁺. The packing of the molecules is such that parallel sheets of the Fo8 are formed (Figure 1 d) through bifurcated hydrogen bonding with CF_3COO^- counterions.

The orientation of the polyether loops with respect to the directionality of the extending triazoles on the xylylene link-

ers may seem, at first glance, to be somewhat unexpected, since the loops do not simply extend from the triazole linkage and thread directly through the cavity of the cyclophane, but rather, the polyether loops fold back around the outside of the cyclophane and enter the cavity from the opposite side with respect to the protruding triazole rings. Inspection of the solid-state structure of *trans*-1-4TFA demonstrates clearly the structure-directing properties of the C–H···O interactions, and it would seem prudent to assume that this particular orientation, stabilized by these noncovalent bonding contacts, is also favored in solution. This conformation maintains the predicted symmetry^[9] assignments and also sheds light on the orientation of the DNP unit inside the cyclophane in solution, in which the oxygen atoms of the DNP unit point away from triazole rings to avoid steric clashes—a point we could not determine with certainty by using any 1D or 2D NMR spectroscopic techniques.

In an effort to establish the ¹H NMR spectroscopic assignments as fully as possible, a symmetry analysis was conducted on each isomer. The *cis* isomer of 1-4PF₆ resides (Figure 2a) in the C₂ point group, that is, it contains only a C₂ axis of rotation. Hence, of the eight protons α to the nitro-

gen atoms of the bipyridinium units, there are four (α₁, α₂, α₃, α₄) heterotopic pairs of homotopic protons. Of the eight protons β to the same nitrogen atoms, there are four (β₁, β₂, β₃, β₄) heterotopic pairs of homotopic protons. Of the six *p*-xylylene protons, there are three (a, b, c) heterotopic pairs of homotopic protons; the two triazole protons are homotopic. Conversely, the *trans* isomer contains only a center of inversion, implying that *trans*-1-4PF₆ resides in the C_i point group (Figure 2b). Thus, of the eight protons α to the bipyridinium nitrogen atoms, there are four (α₁, α₂, α₃, α₄) heterotopic pairs of enantiotopic protons, such that we observe four resonances. Of the eight protons β to these nitrogen atoms, there are four (β₁, β₂, β₃, β₄) heterotopic pairs of enantiotopic protons. Of the six xylene protons, there are three (a, b, c) heterotopic pairs of enantiotopic protons; the two triazole protons are enantiotopic. The result is that each isomer is expected to display nine anisotropic aromatic signals, which is, in fact, what is observed (Figure 2c,d) by ¹H NMR spectroscopy.^[9]

The resulting Fo8 architecture (Figure 3a) resembles, both through topological deformation (Figure 3b) and in appearance, the rose topology (or figure-of-eight, Figure 3c). Although a molecular Fo8 is considered topologically trivial,

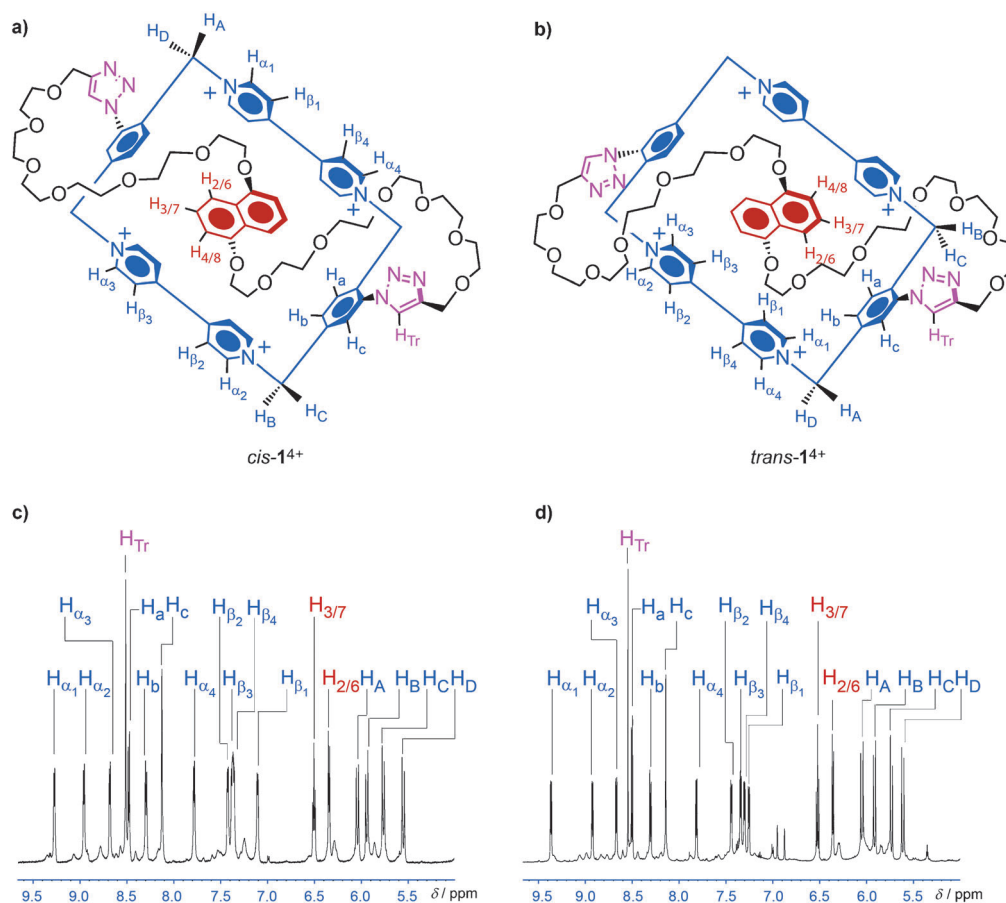


Figure 2. Constitutional isomers of the molecular Fo8 in which a) *cis*-1⁴⁺ is oriented such that both triazoles are pointed toward the same bipyridinium unit and b) *trans*-1⁴⁺ such that the triazoles are pointed toward opposite bipyridinium units. Their corresponding ¹H NMR (600 MHz, CD₃CN, 298 K) spectra are fully assigned as c) *cis*-1-4PF₆ and d) *trans*-1-4PF₆.

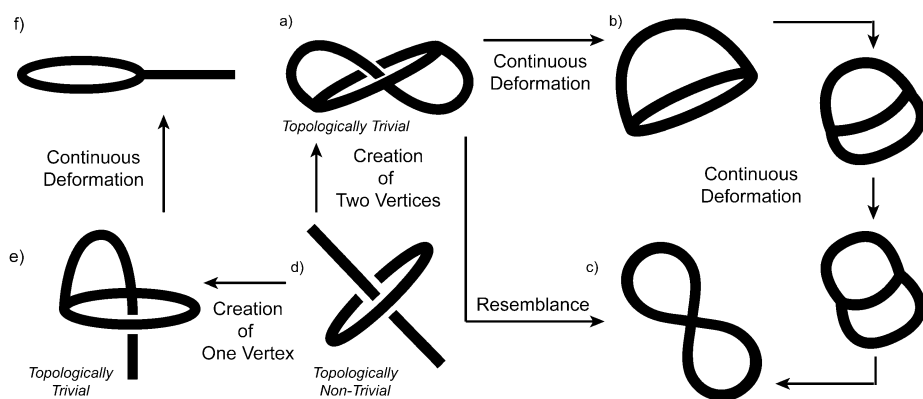


Figure 3. The molecular Fo8 (a) can be deformed continuously through the topology graph (b) to the rose topology (c) at which the self-complexing [1]rotaxane is thus considered homeomorphic to the rose topology containing two petals. Furthermore, the Fo8 can be considered to resemble, even through appearance, the rose topology. In an effort to render the topologically trivial Fo8 onto topologically non-trivial graph, residual topology may be invoked by adding two vertices to a [2]rotaxane in which the thread is considered infinitely long (d).

a residual topological analysis can be conducted to render the Fo8 topologically non-trivial.^[24] Adding vertices to a topologically non-trivial object, instead of rendering their molecular graph more complex, will—most of the time—convert the non-trivial graph to a trivial one, which is indeed the situation we observed with the Fo8. Let us start from a [2]rotaxane that can be considered as non-trivial and identical to a [2]catenane, if we assume that the thread is infinitely long (Figure 3 d). Adding a connection between the ring and the rod leads (Figure 3 e) to a [1]rotaxane. This structure is now trivial because it is identical (Figure 3 f) to a ring bearing a lateral rod. Going further, and now adding two vertices (i.e., two connections between the ring and the rod) yields the molecular Fo8. In the same manner as for the previous [1]rotaxane, this species is trivial. Thus, the conclusion is simple: adding connections (or vertices) can lead to simple (trivial) graphs from non-trivial ones. As a consequence of the way the molecule is generated, it can be considered to have residual topology.^[24]

It also transpires that each isomer occupies two non-degenerate conformations that are in dynamic equilibrium with each other, as evidenced by 2D ¹H NMR experiments in an approximate 9:1 ratio in CD₃CN. In order to study the dynamic equilibria more closely, solutions of one single pure isomer were employed: for this discussion, the *trans* isomer (Figure 4) the structure of which is known in the solid-state will be used to draw conclusions. The same observations and conclusions (see Supporting Information) can be reached in the case of the *cis* isomer. We will consider the major solution species (desig-

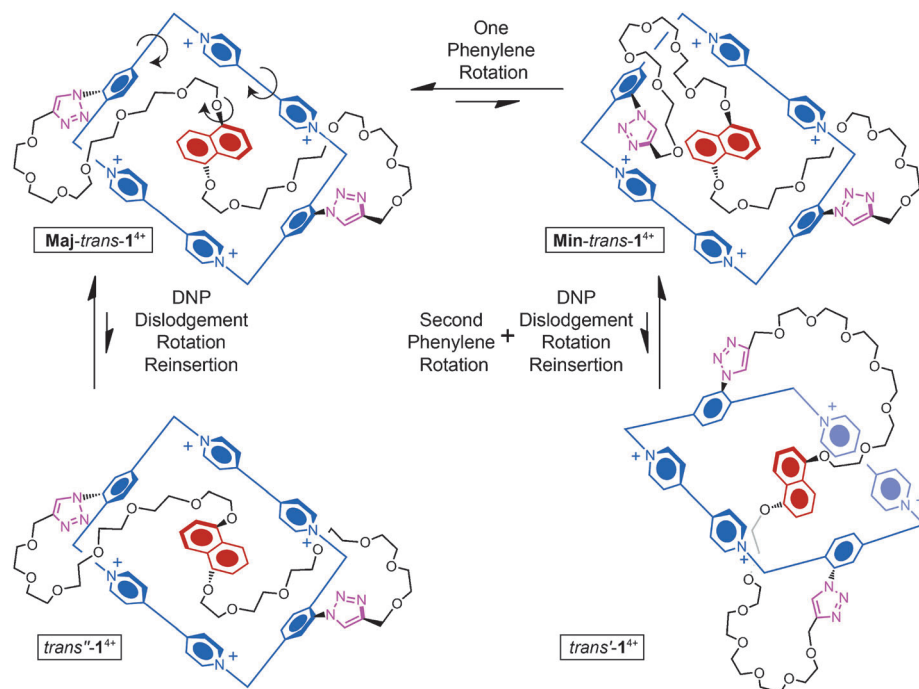


Figure 4. The major conformation **Maj-*trans*-1⁴⁺** as observed in the solid-state structure is expected to undergo three dynamic processes in solution: 1) a process by which a) DNP is dislodged from the cavity, followed by b) a 180° rotation around its [O...O] axis, and c) its reinsertion inside the cavity; 2) pyridinium ring rotation; and 3) phenylene ring rotation. The first process involving the rotation of the DNP unit results in a conformation *trans*'-1⁴⁺ that is predicted to be highly unstable because of multiple steric interactions between the oxygen atoms of the DNP unit and the extending triazole rings. Pyridinium ring rotation does not result in a different conformation, but simply exchanges previously heterotopic protons on the bipyridinium ring and results in new homotopic pairs. Phenylene rotation results in a conformation that is wholly asymmetric and is predicted to be the minor species present in the ¹H NMR spectrum, **Min-*trans*-1⁴⁺**. The major conformation is calculated as the more energetically favorable conformation over **Min-*trans*-1⁴⁺** by 4.5 kcal mol⁻¹ in which one phenylene ring has rotated to introduce steric strain between one appended triazole and the extending DNP oxygen. The remaining conformation *trans*'-1⁴⁺ is not observed by ¹H NMR spectroscopy, but initially was predicted to be the major conformation. This conformation results as a combination of dynamic processes: phenylene ring rotation and DNP dislodgement/rotation/reinsertion and is expected to be highly unstable because of various steric clashes between the triazole rings and the oxygen atoms of the DNP unit.

nated **Maj-trans-1⁴⁺**) as the conformation determined by the solid-state structure and draw conclusions about the unidentified minor conformation (**Min-trans-1⁴⁺**) using ¹H NMR spectroscopy.

Typically, donor–acceptor MIMs, that is, catenanes and rotaxanes, containing DNP units and CBPQT⁴⁺ rings will encounter three dynamic processes: 1) a process by which a) the DNP unit is dislodged from the cavity, followed by b) a 180° rotation around its [O⋯O] axis, and c) its reinsertion inside the cavity;^[25] 2) pyridinium ring rotation; and 3) phenylene ring rotation. Let us first of all consider the process of DNP dislodgement/rotation/reinsertion. The local C_{2h} symmetry of DNP unit imposes two different environments on the modified CBPQT⁴⁺ ring. One DNP orientation—the one present in the solid state—is observed as the major conformation by ¹H NMR spectroscopy. The two orientations—one in which the oxygen atoms of the DNP moiety are pointing towards the triazole rings and one in which they are not—are predicted to be in exchange with each other through a previously described^[25b] DNP dislodgement/rotation/reinsertion process. In all of the previous examples involving an unmodified symmetrical CBPQT⁴⁺ ring, this process is a degenerate one. In the case of the Fo8, however, steric factors governed by the need for the DNP oxygen atoms to be located near the triazoles, render one orientation energetically more favorable than the other one. Reorganization of the DNP unit results in two conformations of **trans-1⁴⁺** that differ in the orientation of the DNP unit inside the cyclophane cavity and are shown in Figure 4—the observed major conformation (**Maj-trans-1⁴⁺**) contains the DNP unit in the cavity, such that its oxygen atoms are pointing away from the triazole rings. The other (**trans'-1⁴⁺**) minor conformation (Figure 4) has the oxygen atoms pointing toward the triazole ring, where significant steric interactions lessen its stability so that **trans'-1⁴⁺** is not observed by ¹H NMR spectroscopy. Although the magnitude of the charge-transfer interaction is likely to be similar for both conformations, it is believed that unfavorable steric contacts between the triazole rings and the oxygen atoms of the DNP units, along with the contorted conformations of the polyether loops, are the primary contributors to this proposed stability difference.

Let us next consider pyridinium ring rotation. Previously, this process has been shown^[25a] to be limited by the energy required to remove the DNP unit from the core of the cyclophane. Furthermore, pyridinium rotation of **Maj-trans-1⁴⁺** is expected to be a degenerate process, whereby the pyridinium protons are exchanged with each other in the following pairs: H_{α2}/H_{α3}, H_{β2}/H_{β3}, H_{α1}/H_{α4}, and H_{β1}/H_{β4}. However, because this rotational barrier is sufficiently high, and although broadening of the resonances for the pyridinium protons of **trans-1-4PF₆** in CD₃CN is observed (Figure 5a) at high temperatures in the ¹H NMR spectra, coalescence was not achieved. Upon performing variable-temperature experiments in CD₃NO₂, significant broadening was also observed at high temperatures. Attempts to observe coalescence of these resonances for the pyridinium protons of

trans-1-4PF₆ at higher temperatures in CD₃SOCD₃ resulted in decomposition of the compound.

Finally, we consider phenylene ring rotation, a process that, in previous examples,^[25a] has been observed in systems of lower symmetry, that is, a modified cyclophane as in our case. The barrier to rotation is typically not as high as that for pyridinium ring rotation. However, the barrier of phenylene ring rotation in a cyclophane containing a DNP guest is higher than that without the guest. In light of this observation, phenylene ring rotations in the Fo8 are expected to occur slowly on the ¹H NMR timescale at temperatures above room temperature. By examining all the different conformations which result from phenylene ring rotation, we have identified three different isomers that should, in fact, result in three different ¹H NMR spectra at low temperatures. Two of these conformations reside in the C_i point group as predicted. **Maj-trans-1⁴⁺** adopts a C_i point group and is observed (Figure 4) in the solid-state structure. The other C_i symmetric conformation, in which both phenylene rings have rotated by 180°, is most likely unstable because of steric interactions between the oxygen atoms of the DNP unit and the triazoles. The remaining conformation—the one in which only one phenylene ring has rotated 180° such that both triazoles are pointing in the same direction with regard to the plane of the cyclophane—contains no symmetry whereby, for example, each of the protons α to the nitrogen atoms are heterotopic to each other, resulting in the expected eight resonances for this set of protons. This number of signals is precisely what should be observed for **Min-trans-1⁴⁺** in the ¹H NMR spectrum, suggesting that this conformation is most likely the one which is observed as the minor isomer by ¹H NMR spectroscopy at low temperatures. This conformation was minimized at the M06L/6-31G* level; the M06L functional has previously been shown^[26] to be an accurate method for studying MIMs containing the CBPQT⁴⁺ ring. This **Min-trans-1⁴⁺** conformation is predicted by DFT calculations to be slightly destabilized (4.5 kcal mol⁻¹), as the rotation of one phenylene ring will likely disrupt only half of the C–H⋯O interactions and create an additional steric interaction between one of the oxygen atoms of DNP and one of the triazoles. As the temperature of the NMR probe is raised, the resonances for **Min-trans-1⁴⁺** are observed to coalesce with those for **Maj-trans-1⁴⁺** at approximately room temperature (Figure 5), at which phenylene ring rotation is sufficiently fast on the NMR timescale to allow the various site-exchange processes to occur.

We also consider here the previously proposed conformation^[9] of **trans-1⁴⁺** in which the polyether loops extend away from the triazole and connect to the DNP unit on the same face of the cyclophane. This conformation (**trans'-1⁴⁺**) can be attained when **Maj-trans-1⁴⁺** undergoes a combination of two phenylene ring rotations and DNP dislodgement/rotation/reinsertion. Gas-phase calculations predict that **trans'-1⁴⁺** is 20.1 kcal mol⁻¹ less stable than the observed major conformation. We now believe that this isomer is not observed because of extensive weakening of the C–H⋯O interactions involving both polyether loops.

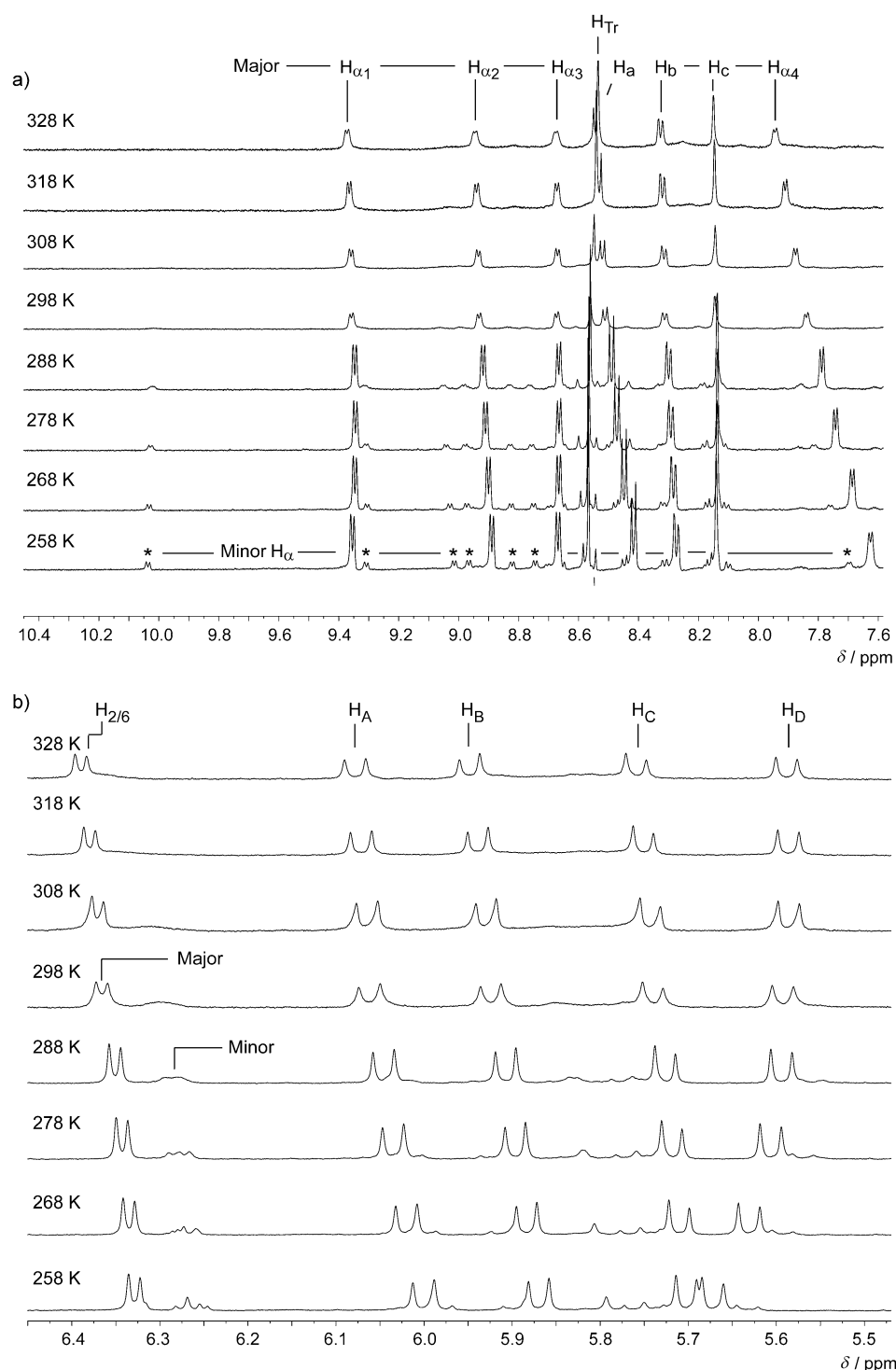


Figure 5. Variable-temperature ^1H NMR (600 MHz, CD_3CN) spectra of a) downfield and b) upfield regions of trans-1.4PF_6 were used to probe the equilibrium processes. The minor species, Min-trans-1^{4+} equilibrates into Maj-trans-1^{4+} at around room temperature. At approximately 328 K, dislodgement of the DNP unit is fast on the NMR timescale, such that pyridinium ring rotation causes the observed broadening (coalescence) of the protons α to the nitrogen atoms of the bipyridiniums.

In an effort to probe the dynamic equilibrium between the two observed conformations (Maj-trans-1^{4+} and Min-trans-1^{4+}) even further, exchange spectroscopy (EXSY) experiments were employed. Exchange peaks are observed,

for example, between the pyridinium protons α to the nitrogen atoms of Min-trans-1^{4+} with Maj-trans-1^{4+} (see Figure S6 in the Supporting Information). These exchange peaks can be rationalized by invoking the process of phenylene ring rotation. We have also used EXSY to probe pyridinium ring rotations and observed that, for example, $\text{H}_{\alpha 1}$ is in exchange with $\text{H}_{\alpha 4}$ by this particular process (Figure S6 in the Supporting Information). Furthermore, in an effort to assign the ^1H NMR spectra of Min-trans-1^{4+} , COSY spectra were employed to identify the protons labeled $\text{H}_{4/8}$. This particular identification of signals at 2.78 ppm verifies that the DNP unit of Min-trans-1^{4+} does in fact lie in the cavity of the cyclophane (Figure S6 in the Supporting Information) as indicated by the strong upfield shift of the $\text{H}_{4/8}$ protons with respect to the corresponding chemical shifts of a free DNP unit.

Conclusion

The use of topological concepts and the application of molecular symmetry arguments are crucial when it comes to identifying the structure and dynamics of higher-order topologies, such as those exemplified by molecular figures-of-eight (Fo8s). Using topological concepts, we have demonstrated the ability to design and synthesize this particular molecular representation of a mathematical topology. Beginning with the synthesis of a bisfunctional, tetracationic electron-deficient cyclophane, subsequent inclusion of an electron-rich guest followed by covalent attachment

of the guest to the host resulted in a pair of subtly different *cis* and *trans* constitutional isomers of a molecular Fo8. Not only was the non-trivial separation and full characterization of these isomers achieved, but also the *cis* and

trans isomers were observed to adopt two different conformations—a major one (**Maj**) and a minor one (**Min**). By utilizing dynamic and 2D ^1H NMR spectroscopic techniques, molecular modeling, and solid-state structural analysis (in one case), two different conformations of Fo8 have been identified and investigated in detail by dynamic ^1H NMR spectroscopy. Furthermore, the solid-state structure of the *trans*-1-4TFA isomer confirms the stereochemistry of the major product. Previously,^[9] without the knowledge of the solid-state structure, and despite our reliance on *ab initio* calculations, we failed to identify the “correct” conformation for the Fo8 compound with respect to the stereochemical relationship between the appendages to the tetracationic cyclophane and the polyether loops joining them to the included 1,5-dioxynaphthalene unit. There is an important lesson to be learned here: it is that no matter how sophisticated molecular modeling, it is foolhardy to believe that 1) computational work alone or 2) computational work which ignores^[27] the experimental evidence will reveal the “correct” scientific answer.

Experimental Section

General methods: Dibromide **7**,^[17] dibromide **9**,^[28] dibromide **13**,^[15a] and 1,5-bis(2-[2-[2-(2-(2-(2-hydroxy)ethoxy)ethoxy)ethoxy]ethoxy]ethoxy)naphthalene^[29] (DNP-HEG-OH) were prepared according to literature procedures. All reagents were purchased from commercial suppliers (Aldrich or Fisher) and used without further purification with the exception of *N*-bromosuccinimide, which was recrystallized from boiling water. Analytical thin-layer chromatography (TLC) was performed on aluminum sheets, precoated with silica gel 60-F254 (Merck 5554). Flash column chromatography was carried out using silica gel 60 (Silicycle) as the stationary phase. Compound purification was performed on a preparative RP-HPLC instrument (Shimadzu LC-8 A), using a C18 column (Agilent, 10 μm packing, 30 mm \times 250 mm). The eluents used were MeCN and H_2O , both mixed with 0.1% (v/v) trifluoroacetic acid (TFA). The detector was set to $\lambda = 254$ nm. Nuclear magnetic resonance (NMR) spectra were recorded at the temperatures noted on Bruker Avance III 500 and 600 MHz spectrometers, with working frequencies of 499.373 and 600.168 MHz for ^1H , and 125.579 and 150.928 MHz for ^{13}C nuclei, respectively. All ^{13}C NMR spectra were recorded with the simultaneous decoupling of ^1H nuclei. Chemical shifts are reported in ppm relative to the signals corresponding to the residual non-deuterated solvents (1.94 ppm for CD_3CN , 7.26 ppm for CHCl_3). Electrospray ionization (ESI) mass spectra were obtained on an Agilent 6210 LC-TOF high-resolution mass spectrometer. Electron Impact (EI) mass spectra were obtained on a Waters GCT Premier mass spectrometer using a Direct Insertion Probe. Crystallographic data were collected at 100 K using a Bruker d8-APEX II CCD diffractometer ($\text{Cu}_{\text{K}\alpha}$ radiation, $\lambda = 1.54178$ Å). Intensity data were collected using ω and ϕ scans spanning at least a hemisphere of reciprocal space for all structures (data were integrated using SAINT^[30]). Absorption effects were corrected on the basis of multiple equivalent reflections (Integration). Structure was solved by direct methods (SHELXS^[30]) and refined by full-matrix least-squares against F^2 (SHELXL^[30]). Hydrogen atoms were assigned riding isotropic displacement parameters and constrained to idealized geometries, including those bound to oxygen, as no hydrogen atoms could be located in the difference Fourier map.

Synthesis of compound 3: 2,5-Dimethylbenzaldehyde (5.00 mL, 35.4 mmol), CBr_4 (23.5 g, 70.8 mmol), and PPh_3 (37.1 g, 142 mmol) were combined in PhMe (100 mL) in a 250 mL round-bottomed flask. The reaction mixture was heated under reflux for 6 h, during which time a white precipitate formed. After cooling, the precipitate was filtered and washed with CH_2Cl_2 . The filtrate was dried (MgSO_4), filtered, and con-

centrated to afford the crude product, which was absorbed on silica gel and purified by column chromatography (SiO_2 , hexanes) to afford **3** as a pure compound (9.03 g, 31.1 mmol) in a 88% yield. ^1H NMR (500 MHz, CDCl_3): $\delta = 7.46$ (s, 1H), 7.22 (s, 1H), 7.07 (m, 2H), 2.33 (s, 3H), 2.23 ppm (s, 3H); ^{13}C NMR (125 MHz, CDCl_3): $\delta = 136.9$, 135.2, 135.1, 132.9, 130.0, 129.2, 129.0, 91.3, 21.0, 19.4 ppm; HR-ESI-MS: m/z calcd for $\text{C}_{10}\text{H}_{10}\text{Br}_2$ [M] $^+$: 287.9149; found: 287.9147.

Synthesis of compound 4: Compound **3** (5.0 g, 17 mmol) was dissolved in anhydrous THF (150 mL) in a 250 mL flame-dried round bottomed flask. The reaction mixture was cooled to -78°C in a dry-ice/ Me_2CO bath and *n*BuLi (15.2 mL of 2.5 M in hexanes, 37.9 mmol) was added dropwise over 30 min. The mixture was stirred for 30 min at -78°C before the lithiate was quenched by the addition of TMSCl (3.28 mL, 25.9 mmol). The mixture was slowly warmed to RT then was left to stir for 16 h before it was quenched with sat. $\text{NH}_4\text{Cl}_{(\text{aq})}$, extracted with CH_2Cl_2 , dried (MgSO_4), filtered, and concentrated to afford the crude product that was absorbed on silica gel and purified by column chromatography (SiO_2 , hexanes) to afford **4** as the pure product (2.02 g, 9.98 mmol) in a 58% yield. ^1H NMR (500 MHz, CDCl_3): $\delta = 7.09$ (s, 1H), 6.89 (d, $^3J = 7.8$ Hz, 1H), 6.84 (d, $^3J = 7.8$ Hz, 1H), 2.22 (s, 3H), 2.10 (s, 3H), 0.09 ppm (s, 9H); ^{13}C NMR (125 MHz, CDCl_3): $\delta = 137.4$, 134.8, 132.5, 129.3, 129.1, 122.5, 104.2, 97.6, 20.6, 20.0, 0.0 ppm; HR-EI-MS: m/z calcd for $\text{C}_{13}\text{H}_{18}\text{Si}$ [M] $^+$: 202.1178; found: 202.1177.

Synthesis of compound 5: Compound **4** (200 mg, 0.988 mmol), *N*-bromosuccinimide (387 mg, 2.17 mmol), and AIBN (8 mg, 0.05 mmol) were dissolved in CCl_4 (10 mL) in a 50 mL round-bottomed flask and the mixture was heated under reflux for 16 h. After cooling to RT, the reaction mixture was washed with H_2O , extracted with CH_2Cl_2 , dried (MgSO_4), filtered, and concentrated to afford the crude product that was absorbed on silica gel and purified by column chromatography (SiO_2 , hexanes) to afford the pure intermediate dibromide as a clear oil (260 mg, 0.721 mmol) in a 73% yield. ^1H NMR (500 MHz, CDCl_3): $\delta = 7.50$ (d, $^3J = 1.8$ Hz, 1H), 7.39 (d, $^3J = 8.0$ Hz, 1H), 7.32 (dd, $^3J = 8.0$ Hz, $^4J = 1.8$ Hz, 1H), 4.64 (s, 2H), 4.42 (s, 2H), 0.29 ppm (s, 9H); ^{13}C NMR (125 MHz, CDCl_3): $\delta = 139.9$, 138.3, 133.3, 130.3, 129.8, 123.7, 101.6, 101.4, 32.3, 31.4, 0.0 ppm. This dibromide (100 mg, 0.278 mmol) and K_2CO_3 (20 mg, 0.139 mmol) were dissolved in a 1:1 THF/MeOH mixture (10 mL) in a 25 mL round-bottomed flask. The reaction mixture was stirred at RT for 3 h while being closely monitored by TLC. The reaction was quenched by the addition of H_2O , extracted with CH_2Cl_2 , dried (MgSO_4), filtered, and concentrated to afford the crude product that was absorbed on silica gel and purified by column chromatography (SiO_2 , hexanes) to afford **5** as the pure compound (46 mg, 0.16 mmol) in a 57% yield. ^1H NMR (500 MHz, CDCl_3): $\delta = 7.56$ (d, $^3J = 1.3$ Hz, 1H), 7.44 (d, $^3J = 8.0$ Hz, 1H), 7.38 (dd, $^3J = 8.0$ Hz, $^4J = 1.3$ Hz, 1H), 4.67 (s, 2H), 4.45 (s, 2H), 3.46 ppm (s, 1H); ^{13}C NMR (125 MHz, CDCl_3): $\delta = 139.9$, 138.2, 133.6, 130.3, 130.0, 122.4, 83.3, 80.1, 31.9, 30.9 ppm; HR-ESI-MS: m/z calcd for $\text{C}_{10}\text{H}_8\text{Br}_2$ [M] $^+$: 285.8993; found: 285.8990.

Synthesis of compound 6-2PF₆: Compound **5** (100 mg, 0.35 mmol) and 4,4'-bipyridine (325 mg, 2.1 mmol) were combined in MeCN (50 mL) and heated under reflux for 12 h. The crude reaction mixture was filtered, the residue dissolved in H_2O (200 mL), and the crude product precipitated by the addition of NH_4PF_6 . Column chromatography (SiO_2 , 2 M $\text{NH}_4\text{Cl}/\text{MeOH}/\text{MeNO}_2$ 12:7:1) was employed to obtain **6-2PF₆** as a pure white solid (190 mg, 0.26 mmol) in a 74% yield. ^1H NMR (CD_3CN , 500 MHz, 293 K): $\delta = 8.85$ (m, 4H), 8.76 (m, 4H), 8.32 (m, 4H), 7.87 (d, $^3J = 6.6$ Hz, 4H), 7.72 (s, 1H), 7.59 (m, 2H), 5.90 (s, 2H), 5.76 (s, 2H), 3.87 ppm (s, 1H); ^{13}C NMR (CD_3CN , 125 MHz, 293 K): $\delta = 155.85$, 152.11, 149.51, 147.99, 146.30, 146.11, 142.00, 136.77, 136.14, 135.09, 132.43, 131.52, 127.36, 127.04, 124.54, 123.55, 122.86, 87.42, 80.02, 73.12, 63.79, 63.16 ppm; HR-ESI-MS: m/z calcd for [M - PF_6] $^+$: 585.1637; found: 585.1652.

Synthesis of compound 8-2PF₆: Dibromide **7**^[17] (120 mg, 0.35 mmol) and 4,4'-bipyridine (325 mg, 2.1 mmol) were combined in MeCN (50 mL) and heated under reflux for 12 h. The crude reaction mixture was filtered, the residue dissolved in H_2O (200 mL), and the crude product precipitated by the addition of NH_4PF_6 . Column chromatography (SiO_2 , 2 M $\text{NH}_4\text{Cl}/\text{MeOH}/\text{MeNO}_2$ 12:7:1) was employed to obtain the product **8-2PF₆** as

a white solid (150 mg, 0.19 mmol) in a 54% yield. $^1\text{H NMR}$ (CD_3CN , 500 MHz, 293 K): δ = 8.86 (m, 4H), 8.75 (d, 3J = 6.7 Hz, 4H), 8.32 (m, 4H), 7.79 (m, 6H), 7.57 (d, 3J = 8.0 Hz, 1H), 6.09 (s, 2H), 5.85 (s, 2H), 4.9 (d, 4J = 2.5 Hz, 2H), 2.85 ppm (t, 4J = 2.5 Hz, 1H); $^{13}\text{C NMR}$ (CD_3CN , 125 MHz, 293 K): δ = 165.72, 155.86, 155.62, 152.14, 152.11, 150.43, 147.12, 146.15, 142.03, 141.97, 136.27, 135.46, 135.38, 134.41, 133.73, 131.02, 127.33, 126.81, 123.03, 122.84, 78.15, 77.16, 63.75, 62.85, 54.31 ppm; HR-ESI-MS: m/z calcd for $[\text{M}-\text{PF}_6]^+$: 643.1703; found: 643.1694.

Synthesis of compound 10: Dibromide **9**^[28] (2.357 g, 6.03 mmol), propargyl bromide (0.676 g, 12.06 mmol), a catalytic amount of pyridinium *p*-toluenesulfonate, and a catalytic amount of 4-dimethylaminopyridine were combined in CH_2Cl_2 (150 mL) at RT. Dicyclohexyl carbodiimide (2.48 g, 12.06 mmol) was added to the CH_2Cl_2 solution and the reaction was left under stirring for 12 h. The crude product was purified by column chromatography (SiO_2 , hexanes/EtOAc) to afford the pure dibromide **10** (2.14 g, 4.99 mmol) in an 82% yield. $^1\text{H NMR}$ (CD_3CN , 500 MHz, 293 K): δ = 7.79 (s, 2H), 4.98 (s, 4H), 4.78 (d, 4J = 2.6 Hz, 2H), 4.45 (s, 2H), 2.84 ppm (t, 4J = 2.6 Hz, 1H); $^{13}\text{C NMR}$ (CD_3CN , 125 MHz, 293 K): δ = 167.9, 167.5, 138.5, 137.7, 129.5, 78.1, 76.8, 54.0, 39.5, 27.1 ppm; HR-ESI-MS: m/z calcd for $\text{C}_{15}\text{H}_{11}\text{O}_4\text{NBr}_2$ $[\text{M}]^+$: 426.9055; found: 426.9042.

Synthesis of compound 11-2PF₆: Dibromide **9** (305 mg, 0.35 mmol) and 4,4'-bipyridine (325 mg, 2.1 mmol) were combined in MeCN (50 mL) and heated under reflux for 12 h. The crude reaction mixture was filtered, the residue dissolved in H_2O (200 mL), and the crude product precipitated by the addition of NH_4PF_6 . Column chromatography (SiO_2 , 2M $\text{NH}_4\text{Cl}/\text{MeOH}/\text{MeNO}_2$ 12:7:1) was employed to afford **11-2PF₆** as a white solid (190 mg, 0.22 mmol) in a 75% yield. $^1\text{H NMR}$ (CD_3CN , 500 MHz, 293 K): δ = 8.86 (m, 8H), 8.33 (d, 2J = 6.4 Hz, 4H), 7.88 (s, 2H), 7.79 (d, 2J = 6.4 Hz, 4H), 6.17 (s, 4H), 4.75 (d, 4J = 2.4 Hz, 2H), 4.45 (s, 2H), 2.85 ppm (t, 4J = 2.4 Hz, 1H); $^{13}\text{C NMR}$ (CD_3CN , 125 MHz, 293 K): δ = 167.7, 167.5, 156.0, 152.0, 146.6, 141.9, 137.8, 133.2, 131.6, 127.0, 122.8, 78.0, 77.0, 59.8, 54.1, 39.7 ppm; HR-ESI-MS: m/z calcd for $[\text{M}-\text{PF}_6]^+$: 725.1705; found: 726.1720.

Synthesis of compound 12: Compound **12** was prepared using a modified procedure developed by Molander et al.^[31] Commercially available 2-bromo-*p*-xylene (30.0 g, 162 mmol), NaN_3 (10.5 g, 162 mmol), CuBr (2.4 g, 16.7 mmol), Cs_2CO_3 (26.4 g, 81 mmol), and *N,N'*-dimethylethylenediamine (2.85 g, 32.3 mmol) were combined in dry DMF (500 mL) and the solution was heated to 90°C with stirring. After 12 h, H_2O (500 mL) was added and the product was extracted with EtOAc (3 × 400 mL). Solvent was removed in vacuo and the product was purified by column chromatography (SiO_2 , hexanes). The fractions containing the product were combined and the solvent was removed in vacuo to yield the azide **12** as a yellow oil (20.5 g, 139 mmol) in a 86% yield. $^1\text{H NMR}$ (CDCl_3 , 500 MHz, 293 K): δ = 7.04 (d, 3J = 7.7 Hz, 1H), 6.93 (s, 1H), 6.85 (d, 3J = 7.7 Hz, 1H), 2.34 (s, 3H), 2.17 ppm (s, 3H). The $^1\text{H NMR}$ spectrum of the product matches that previously reported.^[15a]

Synthesis of compound 13: Compound **12** (294 mg, 2.0 mmol), *N*-bromosuccinimide (764 mg, 4.3 mmol), and AIBN (50 mg, 0.37 mmol) were combined in dry CCl_4 (50 mL) and heated under reflux for 12 h. The mixture was cooled and filtered to remove the insoluble solid. The solvent was then evaporated under reduced pressure and purified by silica gel column chromatography (SiO_2 , CH_2Cl_2 /hexanes 1:6) to give **13**^[15a] as a white solid (310 mg, 0.9 mmol) in a 47% yield. $^1\text{H NMR}$ (500 MHz, CDCl_3 , 298 K): δ = 7.35 (d, 3J = 7.8 Hz, 1H), 7.18 (d, 3J = 1.4 Hz, 1H), 7.14 (dd, 3J = 7.8 Hz, 4J = 1.4 Hz, 1H), 4.47 (s, 2H), 4.46 ppm (s, 2H); $^{13}\text{C NMR}$ (125 MHz, CDCl_3 , 298 K): δ = 138.9, 138.0, 130.7, 127.9, 124.6, 117.9, 30.9, 26.7 ppm; HR-ESI-MS: m/z calcd for $[\text{M}]^+$: 302.9007; found: 302.9001.

Synthesis of compound 14-2PF₆: Dibromide **13**^[15a] (300 mg, 0.9 mmol) and 4,4'-bipyridine (922 mg, 5.9 mmol) were combined in MeCN (50 mL) and heated under reflux for 12 h. The crude reaction mixture was filtered, the residue dissolved in H_2O (200 mL), and the crude product precipitated by the addition of NH_4PF_6 . Column chromatography (SiO_2 , 2M $\text{NH}_4\text{Cl}/\text{MeOH}/\text{MeNO}_2$ 12:7:1) was employed to obtain **14-2PF₆** as a white solid (605 mg, 0.81 mmol) in a 94% yield. $^1\text{H NMR}$ (CD_3CN , 500 MHz, 293 K): δ = 8.86 (m, 8H), 8.33 (d, 3J = 6.9 Hz, 2H), 8.29 (d, 3J =

6.9 Hz, 2H), 7.82 (m, 4H), 7.68 (d, 3J = 7.9 Hz, 1H), 7.51 (d, 3J = 1.4 Hz, 1H), 7.35 (dd, 3J = 7.9 Hz, 4J = 1.4 Hz, 1H), 5.78 (s, 2H), 5.67 ppm (s, 2H); $^{13}\text{C NMR}$ (CD_3CN , 125 MHz, 293 K): δ = 154.2, 153.9, 150.2, 150.1, 144.9, 144.7, 141.6, 141.4, 140.7, 136.2, 135.2, 132.7, 126.0, 125.6, 124.3, 121.9, 121.8, 120.1, 62.7, 59.6 ppm; HR-ESI-MS: m/z calcd for $[\text{M}-\text{PF}_6]^+$: 602.1651; found: 602.1660.

General procedure for cyclophane formation: Precursor salt (0.14 mmol), dibromide (0.14 mmol), and the template—1,5-bis[ethoxy(ethoxy)]dioxynaphthalene (DNP-DEG) (238 mg, 0.41 mmol)—were combined in dry DMF (250 mL) and the solution was stirred at 25°C for 5 days before the solvent was removed in vacuo. The crude reaction mixture was stirred in a saturated aqueous solution of NH_4Cl until the residue dissolved, after which it was diluted with H_2O (ca. 400 mL). Liquid-liquid extraction using CHCl_3 (2 L) was employed to remove the DNP-DEG template (2 days). The remaining crude product was precipitated by the addition of NH_4PF_6 and RP-HPLC was used to attempt to purify the final product. Precursors **6-2PF₆**, **8-2PF₆**, and **11-2PF₆** were utilized in attempts to form tetracationic cyclophanes that failed for the most part.

Synthesis of compound 2-4PF₆: Precursor **14-2PF₆** (120 mg, 0.15 mmol), dibromide **13** (50 mg, 0.15 mmol), and the template DNP-DEG (250 mg, 0.75 mmol) were combined in dry DMF (35 mL), and the solution was stirred at 25°C for 5 days before the solvent was removed in vacuo. The crude reaction mixture was stirred in a saturated aqueous solution of NH_4Cl until the residue dissolved, after which it was diluted with H_2O (ca. 400 mL). Liquid-liquid extraction using CHCl_3 (2 L) was employed to remove the DNP-DEG template (2 days). The remaining crude product was precipitated by the addition of NH_4PF_6 and purified by column chromatography (SiO_2 , 2M $\text{NH}_4\text{Cl}/\text{MeOH}/\text{MeNO}_2$ 12:7:1) to yield the isomeric mixture of bisazides **2-4PF₆** as an off-white solid (45.5 mg, 0.04 mmol) in a 27% yield. $^1\text{H NMR}$ (CD_3CN , 500 MHz, 293 K): δ = 8.90 (m, 8H) 8.17 (m, 8H), 7.65 (d, 3J = 7.81 Hz, 2H), 7.42 (dd, 3J = 7.81 Hz, 4J = 1.55 Hz, 1H), 7.41 (dd, 3J = 7.81 Hz, 4J = 1.55 Hz, 1H), 7.32 (d, 3J = 1.55 Hz, 2H), 5.73 (s, 4H), 5.68 ppm (s, 4H); $^{13}\text{C NMR}$ (CD_3CN , 125 MHz, 293 K): δ = 150.57, 150.46, 146.74, 146.68, 146.20, 146.15, 141.61, 141.57, 138.70, 138.62, 133.60, 133.53, 128.33, 128.27, 127.75, 127.69, 127.10, 127.04, 121.04, 120.98, 65.09, 61.25, 61.22 ppm; ESI-MS: m/z calcd for $[\text{M}-\text{PF}_6]^+$: 1037.1580; found: 1037.1579.

Synthesis of compound 15: NaH (60% in mineral oil, 40 mg, 1 mmol) was added to a solution of DNP-HEG-OH^[29] (185 mg, 0.269 mmol) in dry DMF (20 mL) and stirred for 15 min. Propargyl bromide (80% w/w in PhMe, 0.25 mL, 2.3 mmol) was added slowly, and the mixture stirred for 16 h. MeOH (5 mL) was added carefully to quench remaining NaH, the solvents were removed in vacuo to yield a brown oil, which was purified by column chromatography (SiO_2 , $\text{Me}_2\text{CO}/\text{CH}_2\text{Cl}_2$ 5:95) to yield the product **15** as a light brown oil (137 mg, 0.179 mmol) in a 67% yield. $^1\text{H NMR}$ (CDCl_3 , 500 MHz, 293 K): δ = 7.85 (d, 3J = 8.4 Hz, 2H), 7.34 (t, 3J = 7.8 Hz, 2H), 6.84 (d, 3J = 7.8 Hz, 2H), 4.29 (t, 3J = 5.0 Hz, 4H), 4.19 (d, 3J = 2.4 Hz, 4H), 3.99 (t, 3J = 5.2 Hz, 4H), 3.80 (m, 4H), 3.62–3.71 (m, 18H), 2.43 ppm (t, 3J = 2.3 Hz, 2H); $^{13}\text{C NMR}$ (CDCl_3 , 125 MHz, 293 K): δ = 154.4, 126.9, 125.2, 114.7, 105.7, 79.8, 74.7, 71.1, 70.8, 70.7, 70.7, 70.7, 70.7, 70.0, 69.2, 68.0, 58.5 ppm; ESI-MS: m/z calcd for $[\text{M} + \text{Na}]^+$: 782.4364; found: 782.4340.

Synthesis of figure-of-eight 1-4PF₆: The bisazides **2-4PF₆** (68.3 mg, 0.06 mmol) and guest **15** (39.7 mg, 0.06 mmol) were degassed in DMF (25 mL) with argon before addition of CuI (1.1 mg, 0.006 mmol) and the solution was stirred for 2 days. Solvent was removed in vacuo and the crude product was precipitated from H_2O by the addition of NH_4PF_6 before being purified further using reverse phase high-performance liquid chromatography (RP-HPLC) ($\text{MeCN}/\text{H}_2\text{O}$ 0–40% in 55 min) to yield a pink solid **1-4PF₆** as a mixture of constitutional isomers of (13.0 mg, 0.006 mmol) in a 12% yield. $^1\text{H NMR}$ (CD_3CN , 500 MHz, 293 K): δ = 9.36 (d, 3J = 6.8 Hz, 2H), 9.31 (d, 3J = 6.8 Hz, 2H), 8.97 (d, 3J = 6.8 Hz, 2H), 8.92 (d, 3J = 6.8 Hz, 2H), 8.70 (d, 3J = 6.8 Hz, 2H), 8.67 (d, 3J = 6.8 Hz, 2H), 8.55 (s, 2H), 8.54 (s, 2H), 8.50 (d, 3J = 8.5 Hz, 4H), 8.30 (dd, 3J = 8.5 Hz, 4J = 2.5 Hz, 4H), 8.14 (d, 4J = 2.5 Hz, 7.82 (d, 3J = 6.8 Hz, 2H), 4H), 7.80 (d, 3J = 6.8 Hz, 2H), 7.45 (dd, 4J = 2.4 Hz, 3J = 6.8 Hz, 2H), 7.40 (dd, 4J = 2.4 Hz, 3J = 6.8 Hz, 2H), 7.38 (dd, 4J = 2.4 Hz, 3J = 6.8 Hz, 2H), 7.35 (dd, 4J = 2.4 Hz, 3J = 6.8 Hz, 2H), 7.31 (dd, 4J =

2.4 Hz, $^3J=6.8$ Hz, 2H), 7.26 (dd, $^4J=2.4$ Hz, $^3J=6.8$ Hz, 2H), 7.12 (dd, $^4J=2.4$ Hz, $^3J=6.8$ Hz, 2H), 6.52 (dd, $^3J=7.8$ Hz, $^3J=7.8$ Hz, 2H), 6.51 (dd, $^3J=7.8$ Hz, $^3J=7.8$ Hz, 2H), 6.36 (d, $^3J=7.8$ Hz, 2H), 6.35 (d, $^3J=7.8$ Hz, 2H), 6.05 (d, $^2J=14.7$ Hz, 2H), 6.04 (d, $^2J=14.7$ Hz, 2H), 5.93 (d, $^2J=14.7$ Hz, 2H), 5.91 (d, $^2J=14.7$ Hz, 2H), 5.75 (d, $^2J=14.7$ Hz, 2H), 5.73 (d, $^2J=14.7$ Hz, 2H), 5.59 (d, $^2J=14.7$ Hz, 2H), 5.56 (d, $^2J=14.7$ Hz, 2H), 4.88 (m, 8H), 4.41 (m, 8H), 3.3–3.8 (m, 80H), 3.16 (m, 8H), 2.85 ppm (d, $^3J=7.8$ Hz, 4H); ESI-MS: m/z calcd for $[M-2TFA]^2+$: 796.3169; found: 796.3214. By using iterative RP-HPLC techniques (collection and resubmission through an XBridge Prep C18 OBD 19 × 100 mm column: H₂O/MeCN 0–60% in 60 min $\lambda=254$ nm), the *cis* and *trans* isomers were separated in small quantities for NMR spectroscopic analysis. While the single isomers did not resolve into two different peaks, fractions collected from the RP-HPLC showed increasing enrichment of one isomer and repetitive collection and resubmission allowed for approximately 2 mg of each isomer to be collected.

Crystallographic data for *trans*-1-4TFA: Formula: $[C_{76}H_{90}N_{10}O_{14}(CF_3COO)_4] \cdot 4CH_3CN$; violet plate (0.57 × 0.18 × 0.05 mm); triclinic, $P\bar{1}$, $a=11.083(8)$, $b=14.683(1)$, $c=16.853(2)$ Å, $\alpha=105.73(6)$, $\beta=100.31(6)$, $\gamma=110.62(4)^\circ$, $V=2353.3(3)$ Å³, $Z=1$, $T=100(2)$ K, $\rho_{\text{calcd}}=1.4$ g cm⁻³, $\mu=0.995$ mm⁻¹, $F(000)=1036$. A total of 7860 reflections were collected, of which 5934 were unique, with $R_{\text{int}}=0.1101$. Final $R_1(F^2 > 2\sigma F^2)=0.135$. The atoms of the glycol chain and of the CBPOT⁴⁺ ring showed elongated displacement parameters. Attempts to model this disorder using DFIX and global rigid bond restraints (SIMU/DELU) restraints did not improve the refinement significantly. Hydrogen atoms were refined as riding models with their isotropic displacement parameters linked to their parent atoms. In some cases, the parent atom exhibited disorder with an elongated displacement parameter and therefore the riding hydrogen atom was also large. Portions of the glycol chain were disordered; however, they are bonded to relatively well-ordered parts of the structure. CCDC-867861 contains the supplementary crystallographic data for this paper. These data can be obtained free of charge from The Cambridge Crystallographic Data Centre via www.ccdc.cam.ac.uk/data_request/cif.

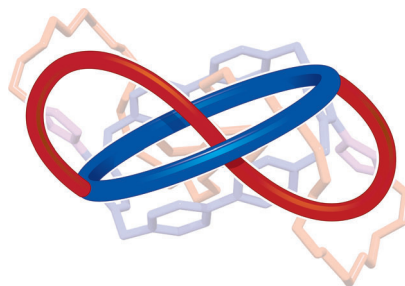
- [1] a) H. L. Frisch, E. Wasserman, *J. Am. Chem. Soc.* **1961**, *83*, 3789–3795; b) S. J. Tauber, *J. Res. Natl. Bur. Stand. Sect. A* **1963**, *67*, 591–599; c) D. M. Walba, *Tetrahedron* **1985**, *41*, 3161–3212; d) D. K. Mitchell, J.-P. Sauvage, *Angew. Chem.* **1988**, *100*, 985–987; *Angew. Chem. Int. Ed. Engl.* **1988**, *27*, 930–931; e) C. O. Dietrich-Buchecker, J.-P. Sauvage, *Angew. Chem.* **1989**, *101*, 192–194; *Angew. Chem. Int. Ed. Engl.* **1989**, *28*, 189–192; f) J. F. Nierengarten, C. O. Dietrich-Buchecker, J.-P. Sauvage, *J. Am. Chem. Soc.* **1994**, *116*, 375–376; g) E. Flapan, *Chaos, Solitons Fractals* **1998**, *9*, 547–560; h) G. A. Breault, C. A. Hunter, P. C. Mayers, *Tetrahedron* **1999**, *55*, 5265–5293; i) E. Flapan, *When Topology Meets Chemistry: A Topological Look at Molecular Chirality*, Cambridge University Press, Cambridge (UK), **2000**; j) J. C. Dobrowolski, *Croat. Chem. Acta* **2003**, *76*, 145–152; k) C. A. Schalley, T. Weilandt, J. Brüggemann, F. Vögtle, *Top. Curr. Chem.* **2005**, *248*, 141–200; l) J. S. Siegel, *Science* **2004**, *304*, 1256–1258; m) C. Dietrich-Buchecker, B. X. Colasson, J.-P. Sauvage, *Top. Curr. Chem.* **2005**, *249*, 261–283; n) E. E. Fenlon, *Eur. J. Org. Chem.* **2008**, 5023–5035; o) D. B. Amabilino, L. Pérez-García, *Chem. Soc. Rev.* **2009**, *38*, 1562–1571; p) R. S. Forgan, J.-P. Sauvage, J. F. Stoddart, *Chem. Rev.* **2011**, *111*, 5434–5464; q) J.-F. Ayme, J. E. Beves, D. A. Leigh, R. T. McBurney, K. Rissanen, D. Schultz, *Nat. Chem.* **2011**, *4*, 15–20.
- [2] a) D. H. Busch, N. A. Stephenson, *Coord. Chem. Rev.* **1990**, *100*, 119–154; b) S. Anderson, H. L. Anderson, J. K. M. Sanders, *Acc. Chem. Res.* **1993**, *26*, 469–475; c) R. Cacciapaglia, L. Mandolins, *Chem. Soc. Rev.* **1993**, *22*, 221–231; d) R. Hoss, F. Vögtle, *Angew. Chem.* **1994**, *106*, 389–398; *Angew. Chem. Int. Ed. Engl.* **1994**, *33*, 375–384; e) J. P. Schneider, J. W. Kelly, *Chem. Rev.* **1995**, *95*, 2169–2187; f) T. J. Hubin, D. H. Busch, *Coord. Chem. Rev.* **2000**, *200*–202, 5–52; g) J. F. Stoddart, H.-R. Tseng, *Proc. Natl. Acad. Sci. USA* **2002**, *99*, 4797–4800; h) F. Aricó, J. D. Badjić, S. J. Cantrill, A. H. Flood, K. C.-F. Leung, Y. Liu, J. F. Stoddart, *Top. Curr. Chem.* **2005**, *249*, 203–259; i) C. D. Meyer, C. S. Joiner, J. F. Stoddart, *Chem. Soc. Rev.* **2007**, *36*, 1705–1723; j) J. D. Crowley, S. M. Goldup, A.-L. Lee, D. A. Leigh, R. T. McBurney, *Chem. Soc. Rev.* **2009**, *38*, 1530–1541.
- [3] a) G. Schill, *Catenanes, Rotaxanes, and Knots*, Academic Press, New York (USA), **1971**; b) *Molecular Catenanes, Rotaxanes and Knots—A Journey Through the World of Molecular Topology*, Wiley-VCH, Weinheim (Germany), **1999**; c) J. F. Stoddart, *Chem. Soc. Rev.* **2009**, *38*, 1802–1820.
- [4] a) P. R. Ashton, T. T. Goodnow, A. E. Kaifer, M. V. Reddington, A. M. Z. Slawin, N. Spencer, J. F. Stoddart, C. Vicent, D. J. Williams, *Angew. Chem.* **1989**, *101*, 1404–1408; *Angew. Chem. Int. Ed. Engl.* **1989**, *28*, 1396–1399; b) J. C. Wang, H. Schwartz, *Biopolymers* **1967**, *5*, 953–966; c) C. Dietrich-Buchecker, J.-P. Sauvage, J.-P. Kintzinger, *Tetrahedron Lett.* **1983**, *24*, 5095–5098; d) M. Cesario, C. O. Dietrich-Buchecker, J. Guilhem, C. Pascard, J.-P. Sauvage, *J. Chem. Soc. Chem. Commun.* **1985**, 244–247; e) C. A. Hunter, *J. Am. Chem. Soc.* **1992**, *114*, 5303–5311; f) F. Vögtle, S. Meier, R. Hoss, *Angew. Chem.* **1992**, *104*, 1628–1631; *Angew. Chem. Int. Ed. Engl.* **1992**, *31*, 1619–1622; g) N. C. Seeman, J. H. Chen, S. M. Du, J. E. Mueller, Y. W. Zhang, T. J. Fu, Y. L. Wang, H. Wang, S. W. Zhang, *New J. Chem.* **1993**, *17*, 739–755; h) M. Fujita, F. Ibukuro, H. Hagihara, K. Ogura, *Nature* **1994**, *367*, 720–723; i) H. Adams, F. J. Carver, C. A. Hunter, *J. Chem. Soc. Chem. Commun.* **1995**, 809–810; j) A. G. Johnston, D. A. Leigh, R. J. Pritchard, M. D. Deegan, *Angew. Chem.* **1995**, *107*, 1327–1331; *Angew. Chem. Int. Ed. Engl.* **1995**, *34*, 1212–1216; k) D. G. Hamilton, J. E. Davies, L. Prodi, J. K. M. Sanders, *Chem. Eur. J.* **1998**, *4*, 608–620; l) D. A. Leigh, P. J. Lusby, S. J. Teat, A. J. Wilson, J. K. Y. Wong, *Angew. Chem.* **2001**, *113*, 1586–1591; *Angew. Chem. Int. Ed.* **2001**, *40*, 1538–1543; m) M. R. Sambrook, P. D. Beer, J. A. Wisner, R. L. Paul, A. R. Cowley, *J. Am. Chem. Soc.* **2004**, *126*, 15364–15365; n) E. N. Guidry, S. J. Cantrill, J. F. Stoddart, R. H. Grubbs, *Org. Lett.* **2005**, *7*, 2129–2132; o) B. Huang, S. M. Santos, V. Felix, P. D. Beer, *Chem. Commun.* **2008**, 4610–4612; p) S. M. Goldup, D. A. Leigh, T. Long, P. R. McGonigal, M. D. Szymes, J. Wu, *J. Am. Chem. Soc.* **2009**, *131*, 15924–15929; q) J. M. Spruell, A. Coskun, D. C. Friedman, R. S. Forgan, A. A. Sarjeant, A. Trabolsi, A. C. Fahrenbach, G. Barin, W. F. Paxton, S. K. Dey, M. A. Olson, D. Benítez, E. Tkatchouk, M. T. Colvin, R. Carmielli, S. T. Caldwell, G. M. Rosair, S. G. Hewage, F. Duclairoir, J. L. Seymour, A. M. Z. Slawin, W. A. Goddard, M. R. Wasielewski, G. Cooke, J. F. Stoddart, *Nat. Chem.* **2010**, *2*, 870–879; r) F. B. L. Coughon, N. A. Jenkins, G. D. Pantoş, J. K. M. Sanders, *Angew. Chem. Int. Ed.* **2012**, *51*, 1443–1447.
- [5] a) P.-L. Anelli, P. R. Ashton, N. Spencer, A. M. Z. Slawin, J. F. Stoddart, D. J. Williams, *Angew. Chem.* **1991**, *103*, 1052–1054; *Angew. Chem. Int. Ed. Engl.* **1991**, *30*, 1036–1039; b) C. Wu, P. R. Lecavalier, Y. X. Shen, H. W. Gibson, *Chem. Mater.* **1991**, *3*, 569–572; c) A. Harada, J. Li, M. Kamachi, *Nature* **1992**, *356*, 325–327; d) R. A. Bissell, E. Córdova, A. E. Kaifer, J. F. Stoddart, *Nature* **1994**, *369*, 133–137; e) P. R. Ashton, R. Ballardini, V. Balzani, M. Bělohorský, M. T. Gandolfi, D. Philp, L. Prodi, F. M. Raymo, M. V. Reddington, N. Spencer, J. F. Stoddart, M. Venturi, D. J. Williams, *J. Am. Chem. Soc.* **1996**, *118*, 4931–4951; f) N. Solladié, J.-C. Chambron, C. O. Dietrich-Buchecker, J.-P. Sauvage, *Angew. Chem.* **1996**, *108*, 957–960; *Angew. Chem. Int. Ed. Engl.* **1996**, *35*, 906–909; g) A. Coskun, D. C. Friedman, H. Li, K. Patel, H. A. Khatib, J. F. Stoddart, *J. Am. Chem. Soc.* **2009**, *131*, 2493–2495.
- [6] K. S. Chichak, S. J. Cantrill, A. R. Pease, S.-H. Chiu, G. W. V. Cave, J. L. Atwood, J. F. Stoddart, *Science* **2004**, *304*, 1308–1312.
- [7] a) Y. Liu, A. H. Flood, R. M. Moskowitz, J. F. Stoddart, *Chem. Eur. J.* **2005**, *11*, 369–385; b) Y. Liu, S. Saha, S. A. Vignon, A. H. Flood, J. F. Stoddart, *Synthesis* **2005**, *18*, 3437–3445.
- [8] Y. Liu, P. A. Bonvallet, S. A. Vignon, S. I. Khan, J. F. Stoddart, *Angew. Chem.* **2005**, *117*, 3110–3115; *Angew. Chem. Int. Ed.* **2005**, *44*, 3050–3055.
- [9] M. M. Boyle, R. S. Forgan, D. C. Friedman, J. J. Gassensmith, R. A. Smaldone, J. F. Stoddart, J.-P. Sauvage, *Chem. Commun.* **2011**, *47*, 11870–11872.

- [10] B. Odell, M. V. Reddington, A. M. Z. Slawin, N. Spencer, J. F. Stoddart, D. J. Williams, *Angew. Chem.* **1988**, *100*, 1605–1608; *Angew. Chem. Int. Ed. Engl.* **1988**, *27*, 1547–1550.
- [11] a) P. R. Ashton, C. L. Brown, E. J. T. Chrystal, T. T. Goodnow, A. E. Kaifer, K. P. Parry, D. Philp, A. M. Z. Slawin, N. Spencer, J. F. Stoddart, D. J. Williams, *J. Chem. Soc. Chem. Commun.* **1991**, 634–639; b) P. R. Ashton, M. Grognoz, A. M. Z. Slawin, J. F. Stoddart, D. J. Williams, *Tetrahedron Lett.* **1991**, *32*, 6235–6238; c) S. Capobianchi, G. Doddi, G. Ercolani, J. W. Keyes, P. Mencarelli, *J. Org. Chem.* **1997**, *62*, 7015–7017; d) G. Cooke, J. F. Garety, S. G. Hewage, B. J. Jordan, G. Rabani, V. M. Rotello, P. Woisel, *Org. Lett.* **2007**, *9*, 481–484; e) S. Nygaard, B. W. Laursen, T. S. Hansen, A. D. Bond, A. H. Flood, J. O. Jeppesen, *Angew. Chem.* **2007**, *119*, 6205–6209; *Angew. Chem. Int. Ed.* **2007**, *46*, 6093–6097.
- [12] M. Asakawa, W. Dehaen, G. L'Abbé, S. Menzer, J. Nouwen, F. M. Raymo, J. F. Stoddart, D. J. Williams, *J. Org. Chem.* **1996**, *61*, 9591–9595.
- [13] Y.-L. Zhao, A. Trabolsi, J. F. Stoddart, *Chem. Commun.* **2009**, 4844–4846.
- [14] M. A. Olson, A. Coskun, L. Fang, A. N. Basuray, J. F. Stoddart, *Angew. Chem.* **2010**, *122*, 3219–3224; *Angew. Chem. Int. Ed.* **2010**, *49*, 3151–3156.
- [15] a) M. A. Olson, A. Coskun, R. Klajn, L. Fang, S. K. Dey, K. P. Browne, B. A. Grzybowski, J. F. Stoddart, *Nano Lett.* **2009**, *9*, 3185–3190; b) R. Klajn, M. A. Olson, P. J. Wesson, L. Fang, A. Coskun, A. Trabolsi, S. Soh, J. F. Stoddart, B. A. Grzybowski, *Nat. Chem.* **2009**, *1*, 733–738.
- [16] C. Reuter, W. Wienand, C. Schmuck, F. Vögtle, *Chem. Eur. J.* **2001**, *7*, 1728–1733.
- [17] A. B. Braunschweig, W. R. Dichtel, O. Š. Miljanić, M. A. Olson, J. M. Spruell, S. I. Khan, J. R. Heath, J. F. Stoddart, *Chem. Asian J.* **2007**, *2*, 634–647.
- [18] a) H. C. Kolb, M. G. Finn, K. B. Sharpless, *Angew. Chem.* **2001**, *113*, 2056–2075; *Angew. Chem. Int. Ed.* **2001**, *40*, 2004–2021; b) C. W. Tornøe, C. Christensen, M. Meldal, *J. Org. Chem.* **2002**, *67*, 3057–3064.
- [19] P. A. S. Smith, J. H. Hall, R. O. Kan, *J. Am. Chem. Soc.* **1962**, *84*, 485–489.
- [20] Two isomers result from the synthesis of **2-4PF₆** where the azides of the cyclophane can either be 1) pointing toward the same bipyridinium (BIPY²⁺) unit (*cis*) or 2) pointing toward opposite BIPY²⁺ units (*trans*). Although the *cis* and *trans* isomers could not be separated, they can be observed separately in the ¹³C NMR spectra with peaks from each isomer shifted from each other by 0.5 ppm.
- [21] Functionalized tetrathiafulvalene compounds present themselves as a mixture of *cis* and *trans* isomers.
- [22] a) Y. H. Jang, S. G. Hwang, Y. H. Kim, S. S. Jang, W. A. Goddard, *J. Am. Chem. Soc.* **2004**, *126*, 12636–12645; b) Y. Liu, S. A. Vignon, X. Zhang, K. N. Houk, J. F. Stoddart, *Chem. Commun.* **2005**, 3927–3929; c) Y. H. Jang, W. A. Goddard, *J. Phys. Chem. B* **2006**, *110*, 7660–7665; d) Q. Li, C.-H. Sue, S. Basu, A. K. Shveyd, W. Zhang, G. Barin, L. Fang, A. A. Sarjeant, J. F. Stoddart, O. M. Yaghi, *Angew. Chem.* **2010**, *122*, 6903–6907; *Angew. Chem. Int. Ed.* **2010**, *49*, 6751–6755; e) C.-H. Sue, S. Basu, A. C. Fahrenbach, A. K. Shveyd, S. K. Dey, Y. Y. Botros, J. F. Stoddart, *Chem. Sci.* **2010**, *1*, 119–125.
- [23] a) K. N. Houk, S. Menzer, S. P. Newton, F. M. Raymo, J. F. Stoddart, D. J. Williams, *J. Am. Chem. Soc.* **1999**, *121*, 1479–1487; b) F. M. Raymo, M. D. Bartberger, K. N. Houk, J. F. Stoddart, *J. Am. Chem. Soc.* **2001**, *123*, 9264–9267.
- [24] O. Lukin, A. Godt, F. Vögtle, *Chem. Eur. J.* **2004**, *10*, 1878–1883.
- [25] a) S. A. Vignon, J. F. Stoddart, *Collect. Czech. Chem. Commun.* **2005**, *70*, 1493–1576; b) M. Asakawa, P. R. Ashton, S. E. Boyd, C. L. Brown, R. E. Gillard, O. Kocian, F. M. Raymo, J. F. Stoddart, M. S. Tolley, A. J. P. White, D. J. Williams, *J. Org. Chem.* **1997**, *62*, 26–37.
- [26] D. Benítez, E. Tkatchouk, I. Yoon, J. F. Stoddart, W. A. Goddard, *J. Am. Chem. Soc.* **2008**, *130*, 14928–14929.
- [27] B. Tejerina, C. M. Gothard, B. A. Grzybowski, *Chem. Eur. J.* **2012**, *18*, 5606–5611.
- [28] Y. Liu, A. H. Flood, J. F. Stoddart, *J. Am. Chem. Soc.* **2004**, *126*, 9150–9151.
- [29] A. J. Zych, B. L. Iverson, *J. Am. Chem. Soc.* **2000**, *122*, 8898–8909.
- [30] G. Sheldrick, *Acta Crystallogr. Sect. A* **2008**, *64*, 112–122.
- [31] Y. A. Cho, D.-S. Kim, H. R. Ahn, B. Canturk, G. A. Molander, J. Ham, *Org. Lett.* **2009**, *11*, 4330–4333.

Received: June 11, 2012

Published online: ■ ■ ■, 0000

The use of topological concepts and the application of molecular symmetry arguments are crucial when it comes to identifying the structure and dynamics of higher-order topologies, such as those exemplified by molecular figures-of-eight. Using topological concepts, the ability to design and synthesize this particular molecular representation of a mathematical topology has been demonstrated.



Topology

*M. M. Boyle, J. J. Gassensmith,
A. C. Whalley, R. S. Forgan,
R. A. Smaldone, K. J. Hartlieb,
A. K. Blackburn, J.-P. Sauvage,*
J. F. Stoddart**



Stereochemistry of Molecular Figures-



of-Eight